Technical Report

R 845

July 1976

CIVIL ENGINEERING LABORATORY
Naval Construction Battalion Center
Port Hueneme, California 93043

ICE ENGINEERING - A HEAT SINK METHOD FOR SUBSURFACE ICE THICKENING

by J. L. Barthelemy

Sponsored by

NAVAL FACILITIES ENGINEERING COMMAND

Unclassified

SECURITY CLASSIFICATION OF THIS PAGE *(When Data Entered)*

REPORT DOCUMENTATION PAGE		READ INSTRUCTIONS BEFORE COMPLETING FORM
1. REPORT NUMBER TR-845	2. GOVT ACCESSION NO. DN144029	3. RECIPIENT'S CATALOG NUMBER
4. TITLE *(and Subtitle)* ICE ENGINEERING – A HEAT SINK METHOD FOR SUBSURFACE ICE THICKENING		5. TYPE OF REPORT & PERIOD COVERED Final; June 1969 to June 1975 6. PERFORMING ORG. REPORT NUMBER
7. AUTHOR(s) J. L. Barthelemy		8. CONTRACT OR GRANT NUMBER(s)
9. PERFORMING ORGANIZATION NAME AND ADDRESS Civil Engineering Laboratory Naval Construction Battalion Center Port Hueneme, California 93043		10. PROGRAM ELEMENT, PROJECT, TASK AREA & WORK UNIT NUMBERS 62759N; YF52.555.002.01.003
11. CONTROLLING OFFICE NAME AND ADDRESS Naval Facilities Engineering Command Alexandria, Virginia 22332		12. REPORT DATE July 1976 13. NUMBER OF PAGES 27
14. MONITORING AGENCY NAME & ADDRESS*(if different from Controlling Office)*		15. SECURITY CLASS. *(of this report)* Unclassified 15a. DECLASSIFICATION/DOWNGRADING SCHEDULE

16. DISTRIBUTION STATEMENT *(of this Report)*

Approved for public release; distribution unlimited.

17. DISTRIBUTION STATEMENT *(of the abstract entered in Block 20, if different from Report)*

18. SUPPLEMENTARY NOTES

19. KEY WORDS *(Continue on reverse side if necessary and identify by block number)*

Ice engineering, subsurface ice thickening, natural convection heat exchanger, freezing cells, effective heat sink, ambient heat sink.

20. ABSTRACT *(Continue on reverse side if necessary and identify by block number)*

Ice sheets are being used as runways and as roadbeds for aircraft and heavy-haul transportation vehicles in the Arctic and Antarctic. Thin ice often makes operations on the ice sheets costly and dangerous. The Civil Engineering Laboratory has developed methods of freezing seawater at coastal polar locations to thicken natural ice formations into useful platform foundations. This report documents the process of thickening ice

continued

DD FORM 1 JAN 73 1473 EDITION OF 1 NOV 65 IS OBSOLETE

Unclassified

SECURITY CLASSIFICATION OF THIS PAGE *(When Data Entered)*

20. Continued

by the use of freezing cells to accelerate ice growth on the underside of an ice sheet. The freezing cell described in this report is driven by density differences: liquid above is cooled by the air, and liquid below is warmed by the seawater medium.

Library Card

Civil Engineering Laboratory
ICE ENGINEERING – A HEAT SINK METHOD FOR SUBSURFACE ICE THICKENING (Final), by
J. L. Barthelemy
TR-845 27 pp illus July 1976 Unclassified

1. Ice sheet thickening 2. Freezing cells I. YF52.555.002.01.003

Ice sheets are being used as runways and as roadbeds for aircraft and heavy-haul transportation vehicles in the Arctic and Antarctic. Thin ice often makes operations on the ice sheets costly and dangerous. The Civil Engineering Laboratory has developed methods of freezing seawater at coastal polar locations to thicken natural ice formations into useful platform foundations. This report documents the process of thickening ice by the use of freezing cells to accelerate ice growth on the underside of an ice sheet. The freezing cell described in this report is driven by density differences: liquid above is cooled by the air, and liquid below is warmed by the seawater medium.

INTRODUCTION

In accordance with international treaty policy, naval activities in the Antarctic are confined to a role of assistance: the Navy provides vital supply and logistic functions in support of scientific and research programs. At the top of the world, naval interests are geared more toward ensuring the integrity of the northern frontier. The Arctic Ocean, the world's fourth largest body of water, is enclosed almost entirely by land masses and strategically links North America, Greenland, Europe, and Asia. The recent discovery and exploitation of large gas and oil reserves in Alaska and Canada have given this area even greater importance.

One important aspect of polar activity involves on-the-ice logistics. Historically, frozen waters have been used in both the Arctic and Antarctic to support movement of men, equipment, and supplies. Ice sheets have been used extensively as runways for aircraft and as roadbeds for heavy-haul transportation vehicles. Prior to 1966, for instance, ships supplying McMurdo Station, the major United States base in the Antarctic, unloaded cargo directly onto the winter ice sheet at some distance from shore. Unfortunately, thin ice often rendered that operation very costly and dangerous [1]. To counter such problems, the Civil Engineering Laboratory (CEL) developed methods of freezing seawater at coastal polar locations to thicken natural ice formations into useful platform foundations. This report documents the process of subsurface ice thickening — a technique used to accelerate ice growth at the underside of an ice sheet.

BACKGROUND

The hostile and desolate environment encountered in polar regions presents man with many problems atypical to other parts of the world. Winter climatic conditions are severe, characterized by periods of total darkness, low temperatures, and strong winds. Outside work is accomplished only with great effort and hardship, and very few readily usable resources are available. Supplies, equipment, and construction materials must be transported at great expense by ship or airplane. As a result, construction by conventional means is often unfeasible. Mankind, however, has an uncanny ability to adapt to the surrounding environment, changing obstacles to potential assets. Just as the Eskimos have utilized ice for housing and shelter, so the Navy is developing techniques and equipment to increase the usefulness of this abundant material. Unlike the Eskimo, however, who cut and moved existing ice formations, the Navy is studying localized freezing of seawater to increase the strength of natural ice formations.

The insulating property of an advancing ice sheet retards additional growth, thereby limiting the thickness that can be achieved during a single winter season. It is often necessary to increase thickness for added strength before an annual ice sheet can be used to support heavy equipment or temporary facilities. Surface flooding techniques developed by CEL have produced layered ice thickening by intermittent flooding and freezing of the surface of an annual ice sheet with subsurface seawater [2-5]. That method is generally useful for producing large, flat expanses of thickened ice. However, it is deficient in several ways: (1) localized deflections around the pump discharge limit the outward spread of flood water unless an initial natural ice thickness of 2 to 3 feet is used; (2) the performance of men and the operation of equipment are seriously handicapped by inclement weather; and (3) habitats and maintenance facilities must be provided for long-term housing of men and equipment.

An alternative scheme accelerates ice growth at the underside of an existing ice sheet. Most simply, pipes with closed ends and containing a subfreezing refrigerant are installed through an ice sheet into the waters below, thereby promoting subsurface, radial ice growth. These pipes effectively short-circuit the insulating tendency of the ice sheet. Heat transfer from seawater to ambient air is redirected by means of a natural convection recirculating cycle within the

pipe: the heat of fusion is extracted from the seawater by the cold refrigerant and then rejected by the refrigerant to the colder atmosphere. The recirculating cycle is a result of density differences within the liquid refrigerant. Therefore, such a cooling device is irreversible, operating only during those periods when the ambient air is at a temperature lower than the subsurface seawater.

The self-powered heat exchanger is driven by temperature inversion and is called a "freezing cell" when used in polar application to thicken ice sheets. It should be noted, however, that the concept of a self-regulated heat exchanger is not new in polar regions; only the application is new. Two types of devices for ground cooling have been used for some time in Alaska and Canada to stabilize piling in permafrost. Externally, the two types are similar in construction, consisting most simply of a closed-end pipe positioned vertically such that part of it is exposed to the cold air and part is embedded in the unstable ground. The above-ground cooling head is often fitted with fins to facilitate heat rejection.

Internally, they operate differently. One type (the Batch pile) employs liquid convection and is driven by density differences: liquid above is cooled by the air, and liquid below is warmed by the soil. The two-phase vapor system (the Long pile) requires a fluid with a low boiling temperature: liquid in the lower section of the heat exchanger vaporizes and rises to the cooling head, where it condenses to repeat the process.

All freezing cells analyzed and tested by CEL have been of the liquid convection type. Therefore, reference in this report to a freezing cell is synonymous with reference to a self-powered heat exchanger similar in operation to the Balch pile. Figure 1 presents a typical device.

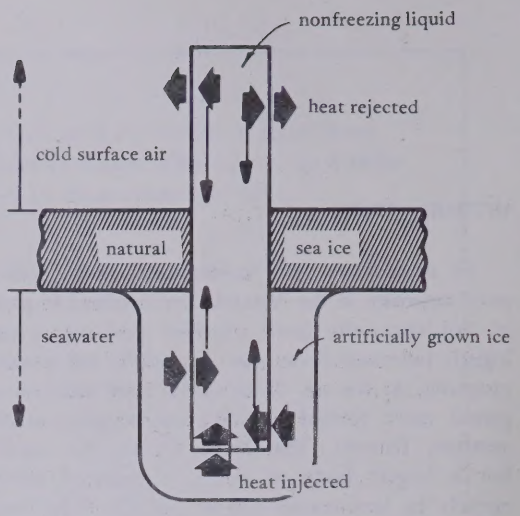

Figure 1. Liquid-convection ice-thickening device.

ANALYSIS

Freezing cells have several operating characteristics that are especially attractive for ice thickening:

1. Maximum heat transfer takes place under the worst climatic conditions. During the winter months of total darkness, the heat input due to solar radiation is zero. Low ambient air temperatures coupled with high wind velocities serve to maximize the chill factor and, thus, the driving potential.

2. In addition to being self-powered, these systems have the added advantage of requiring minimum personnel and equipment during installation and require little, if any, maintenance.

3. They may be installed at the area of minimum ice thickness necessary to support the placement crew and ice-coring equipment.

Qualitative

The mathematical prediction of radial ice growth is derived in terms of the ambient heat sink and design characteristics of freezing cell. The following assumptions are made to facilitate the development:

1. The seawater medium is at its freezing-point temperature.

2. Freezing cells operate only when the ambient air temperature is lower than the freezing point of seawater.

3. The thermal properties of seawater ice are uniform and temperature invariant.

4. Heat capacity of the subcooled ice is negligible relative to the latent heat of solidification.

5. The bulk temperature of the liquid refrigerant is uniform throughout the freezing cell at any time.

6. Thermal lag due to capacitance effects in the liquid and ice shell can be ignored if performance is modeled after the total heat sink rather than an exact temperature-time relationship.

The following rationale was used to justify the above assumptions:

1. During the winter months in which an annual ice sheet develops, the seawater surrounding many polar locations is at the freezing point temperature. This condition prevails along the strategically important north coast of Alaska and in the Ross Sea, Antarctica [6].

2. Freezing cells are irreversible devices driven by density differences within the refrigerant, which is cooled above and heated below. When temperature inversion ceases, heat transfer does not continue.

3. Thermal properties of seawater ice do not vary appreciably within the temperature range typical of polar ice sheets.

4. Seban [7] has demonstrated that specific heat effects are not appreciable when the parameter $L/C\Delta T$, which expresses the ratio of fusion energy to stored energy, is larger than 1.5. For freezing cells, this parameter is more on the order of 10 or greater.

5. In most instances, natural convection effects are limited to a thin film at the inside area of the cell. The bulk of the refrigerant is nearly isothermal.

6. Under actual field conditions, ambient air temperatures fluctuate with the passage of time. Refrigerant temperatures do not trace the pattern of air temperatures exactly because of thermal lag: freezing cell response delays and dampens oscillations recorded in air temperatures.

However, analysis of ice growth does not require an exact description of the time-temperature interaction; but, rather, thickness can be approximated for engineering purposes in terms of net energy withdrawal. In this report, the degree-day concept is used to compute heat transfer from the seawater medium. The independent variable is the heat sink — that is, the accumulation of degrees of temperature below freezing for given periods of time. When the ambient temperature varies with time over a period of interest, the time-averaged value of ambient temperature can be used rigorously since the instantaneous freezing rate is directly proportional to the overall temperature difference. Thus, the integrated number of degree-days

$$\int_0^t [T_\lambda - T_a(t)]\, dt$$

can be alternately represented by

$$[T_\lambda - \overline{T_a(t)}]\, t$$

where $\overline{T_a(t)}$ is the time-averaged ambient temperature evaluated for the period of interest. This quantity is the "ambient heat sink," the maximum heat sink available to a freezing cell. Of course, ice production is directly related to the temperature along the subsurface section of the freezing cell, and this pipe temperature will not be as cold as the surface air. Therefore, the entire ambient heat sink is not utilized for ice production. That portion that is used is designated the "effective heat sink." This quantity is written in terms of degree-days as a function of the time-averaged pipe temperature over the same period of interest

$$[T_\lambda - \overline{T_i(t)}]\, t$$

By considering heat transfer in terms of steadily applied average temperatures, one conveniently idealizes a model in which thermal lag due to capacitance effects is effectively removed.

The colder the operating temperature of a freezing cell, the greater will be the capacity for ice production. Of course, the greatest possible heat sink is that of the cold ambient environment. A useful concept in freezing cell analysis is that of the perfect cell (that is, one so constructed that the liquid refrigerant temperature is always as cold as the ambient air). Such a device may be said to have 100% conversion efficiency in that it utilizes the total ambient heat sink for ice growth. In actual fact, the freezing cell is a resistance device, and the operating

temperature is determined by a balance of thermal resistances. Only a part of the ambient heat sink is effectively utilized. When air temperature data are known, perfect-cell analysis predicts maximum ice growth. Other cells are rated according to their heat-sink conversion characteristics.

Quantitative

Figure 2 presents in cross section a pipe with growing ice shell. In problems involving solidification, the pertinent heat conduction relationships embody the constraint that the liquid-solid interface must move with a velocity proportional to the rate with which heat is withdrawn from that interface. Since specific heat changes are neglected, an energy balance at the interface reveals that the inward flow of heat due to conduction is equal to the heat of fusion extracted from an incremental extension in thickness.

Equation Development.

$$(\rho L)_i \frac{dr_o}{dt} = k_i \frac{dT}{dr}\Big|_{r=r_o} \qquad (1)$$

Heat transfer is modeled after a gradually changing, time-averaged pipe temperature. The temperature profile within the growing ice shell is approximated by that of steady-state conduction through a hollow cylinder. At each instant in time

$$T(r,t) = \overline{T_i(t)} + [T_\lambda - \overline{T_i(t)}] \frac{\ln(r/r_i)}{\ln(r_o/r_i)} \qquad (2)$$

Differentiation of Equation 2 and evaluation at r_o yields

$$\frac{dT}{dr}\Big|_{r=r_o} = \frac{T_\lambda - \overline{T_i(t)}}{r_o \ln(r_o/r_i)} \qquad (3)$$

which, upon substitution into Equation 1, gives

$$\frac{dr_o}{dt} = \frac{\alpha[T_\lambda - \overline{T_i(t)}]}{r_o \ln(r_o/r_i)} \qquad (4)$$

The thermal properties of ice have been grouped into the ice property constant α, where, by definition,*

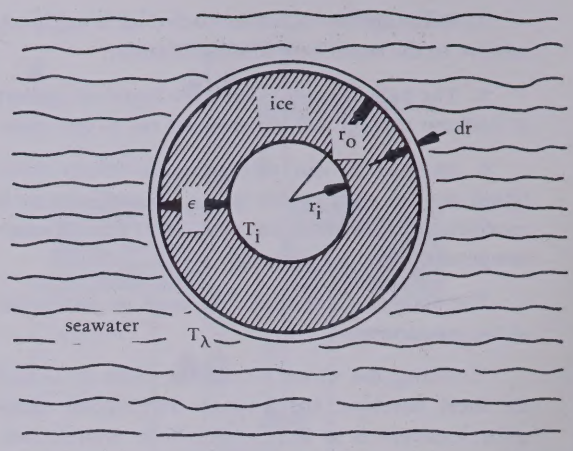

Figure 2. Cross section of radial ice growth around pipe in seawater.

$$\alpha = \left(\frac{k}{\rho L}\right)$$

Equation 4 demonstrates the manner in which the radial growth rate decreases with increased ice thickness. To express this relationship non-dimensionally in terms of heat sink, the following transformations are made:

$$R = \frac{r_o}{r_i} \qquad (5)$$

$$\omega = \frac{\alpha}{r_i^2} [T_\lambda - \overline{T_i(t)}]\, t \qquad (6)$$

The variable ω is a dimensionless representation of the effective heat sink, hereupon referred to as the generalized effective heat sink. Upon substitution, Equation 4 becomes

$$\frac{dR}{d\omega} = \frac{1}{R \ln(R)} \qquad (7)$$

Equation 7 can be integrated by separating variables such that

$$\omega = \int_1^R [\xi \ln(\xi)]\, d\xi \qquad (8)$$

*In Reference 6, the ice property constant was defined as $\alpha = \sqrt{(k/\rho L)_i}$. For clarity, the constant is redefined in this report.

where ξ is a dummy variable introduced for integration. Integration of the right-hand side yields

$$\omega = \frac{1}{2} R^2 \left[\ln(R) - \frac{1}{2} \right] + \frac{1}{4} \qquad (9)$$

The constant of integration (1/4) is significant only for small values of R; it may be neglected. Also, generalized ice thickness ($\phi = R - 1$) is a more meaningful parameter than the radius ratio. The working form of Equation 9 is written as follows:

$$\omega = \frac{1}{2} (\phi + 1)^2 \left[\ln(\phi + 1) - \frac{1}{2} \right] \qquad (10)$$

The left-hand side is a dimensionless measure of the total heat conducted from the seawater, and the right-hand side represents the ice thickness resulting from the energy withdrawal.

Equation 10 presents the functional relationship between effective heat sink and radial ice thickness. However, as is obvious from Equation 6, evaluation of the effective heat sink requires a knowledge of thermal history of the freezing cell (subsurface) pipe. Pipe temperature, in turn, is a function of ambient air temperature and heat exchanger design. In other words, although Equation 10 is convenient for calculating ice thickness when pipe temperatures are monitored, it does not provide a method for predicting ice production in advance of actual operation. Thus, it is more practical to define ice growth as a function of the ambient heat sink. When this is done, ice thickness for a freezing cell of specific design can be forecast directly in terms of typical or anticipated air temperatures.

The ambient heat sink is made dimensionless by use of the following transformation:

$$\Omega = \frac{\alpha}{r_i^2} [T_\lambda - \overline{T_a(t)}] t \qquad (11)$$

This parameter is called the generalized ambient heat sink. Since the overall temperature potential is the difference between the seawater and air temperatures, and the effective potential is the difference between the seawater and pipe temperatures, that fraction of the maximum heat sink being utilized at any instant of time for ice growth is equal to the ratio of potentials such that

$$\frac{d\omega}{d\Omega} = \frac{T_\lambda - \overline{T_i(t)}}{T_\lambda - \overline{T_a(t)}} \qquad (12)$$

The value of this ratio is time dependent; it is determined by a thermal-resistance balance that changes constantly due to continuous thickening of the insulating ice shell. In effect, Equation 12 is a measure of heat exchanger efficiency; it shows what fraction of the ambient heat sink is being converted at any given point in time. This ratio is defined as conversion efficiency and will be designated by the variable θ. Thus, by definition,

$$\theta(t) = \frac{T_\lambda - \overline{T_i(t)}}{T_\lambda - \overline{T_a(t)}} \qquad (13)$$

Substitution of Equations 12 and 13 into Equation 7 gives the dimensionless ice growth rate in terms of the ambient heat sink

$$\frac{dR}{d\Omega} = \frac{\theta(t)}{R \ln(R)} \qquad (14)$$

However, Equation 14 cannot be integrated until the functional form of conversion efficiency is established. This is accomplished by analyzing the heat transfer problem in terms of a network of thermal resistance.

Electrical Analogue. The electrical analogue to the simplified freezing cell model is presented in Figure 3. The overall potential at a point in time is the difference between the seawater and average air temperatures. The effective potential is the difference between seawater and average pipe temperatures. There are four thermal resistances: (1) R_i is the result of the growing ice shell and is therefore variable; (2) R_1 is the natural convection resistance (within the freezing cell) due to refrigerant warming; (3) R_2 is the natural convection resistance due to refrigerant cooling; and (4) R_a is the convective resistance (at the outside of the cooling head) due to heat rejection to the air.

The model analogue is composed of thermal resistance only. Therefore, by continuity of heat flow,

$$\frac{T_\lambda - \overline{T_i(t)}}{R_i} = \frac{T_\lambda - \overline{T_a(t)}}{R_i + R_1 + R_2 + R_a} \qquad (15)$$

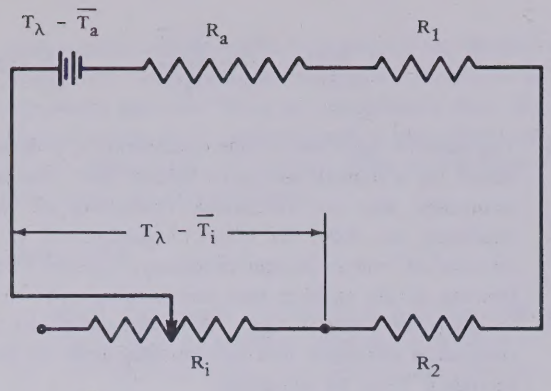

Figure 3. Electrical analogue to freezing cell model.

Rearranging,

$$\theta(t) = \frac{1}{1 + \dfrac{R_1 + R_2 + R_a}{R_i}} \tag{16}$$

Conversion efficiency is thus dependent on the ratio of resistance. As ice thickness increases, $\theta(t)$ approaches unity.

The thermal resistance of the growing ice shell is that associated with the radial flow of heat being conducted through a hollow circular cylinder. It is written in the form

$$R_i = \left(\frac{r}{k\,A}\right)_i \ln(R) \tag{17}$$

The other three resistances are characteristics of the freezing cell itself. As is standard practice in heat exchanger analysis, their sum is written in terms of a characteristic surface area and an overall heat transfer coefficient that combines the effects of conduction and convection. In this study, the characteristic area is the total heat rejection surface (including fins) of the cooling head. Thus, by definition

$$R_1 + R_2 + R_a = \frac{1}{h\,A_a} \tag{18}$$

To be consistent with previous equation development, the overall heat transfer coefficient h is made nondimensional. The following transformation is made

$$h^* = \left(\frac{r}{k}\right)_i h\,A^* \tag{19}$$

where

$$A^* = \frac{A_a}{A_i} \tag{20}$$

The parameter h^* is a dimensionless representation of the overall heat transfer coefficient. It is called "generalized conductance" and contains those design properties that determine conversion efficiency. Substitution of Equations 17 through 20 into Equation 16 gives

$$\theta(t) = \frac{1}{1 + \dfrac{1}{h^* \ln(R)}} \tag{21}$$

Equation 21 provides the working relationship for conversion efficiency in terms of heat transfer performance and design. Thus, Equation 14 may be separating the variables, and substituting in the relationship for conversion efficiency,

$$d\Omega = \left[R \ln(R) + \frac{R}{h^*}\right] dR \tag{22}$$

Finally,

$$\Omega = \int_1^R \left[\xi \ln(\xi) + \frac{\xi}{h^*}\right] d\xi \tag{23}$$

As previously, the constant of integration is neglected, and generalized thickness ϕ is introduced to replace the radius ratio. The final product of integration and simplification is

$$\Omega = \frac{1}{2}(\phi + 1)^2 \left[\ln(\phi + 1) - \frac{1}{2}\right] + \frac{\phi(\phi + 2)}{2h^*} \tag{24}$$

Equation 24 provides the desired working relationship: ice thickness is expressed as an implicit function of the ambient heat sink and generalized conductance. Figure 4 presents the family of curves plotted from Equation 24. Figure 5 demonstrates the dependence of conversion efficiency on generalized conductance and length of time in service.

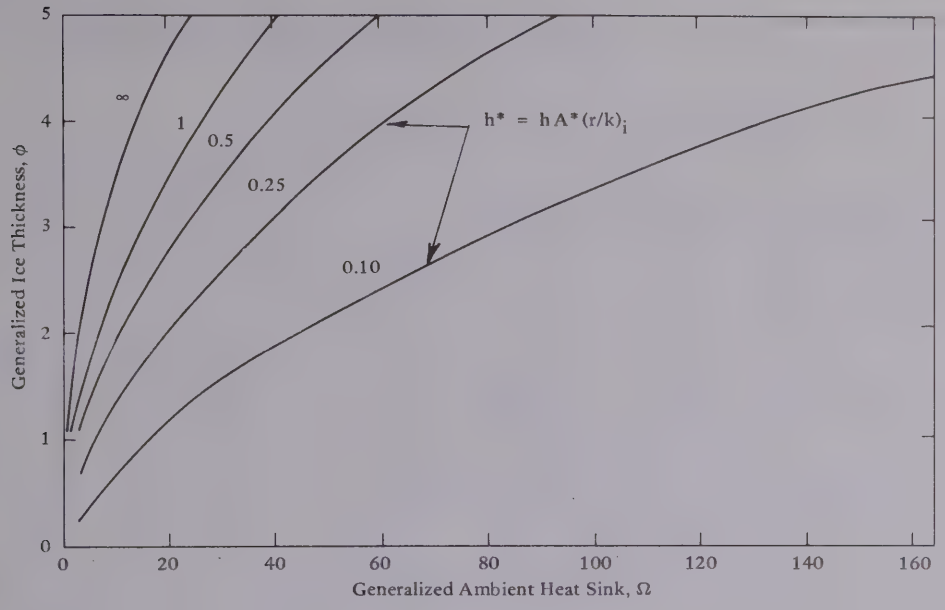

Figure 4. Radial growth of ice around a freezing cell in terms of dimensionless moduli.

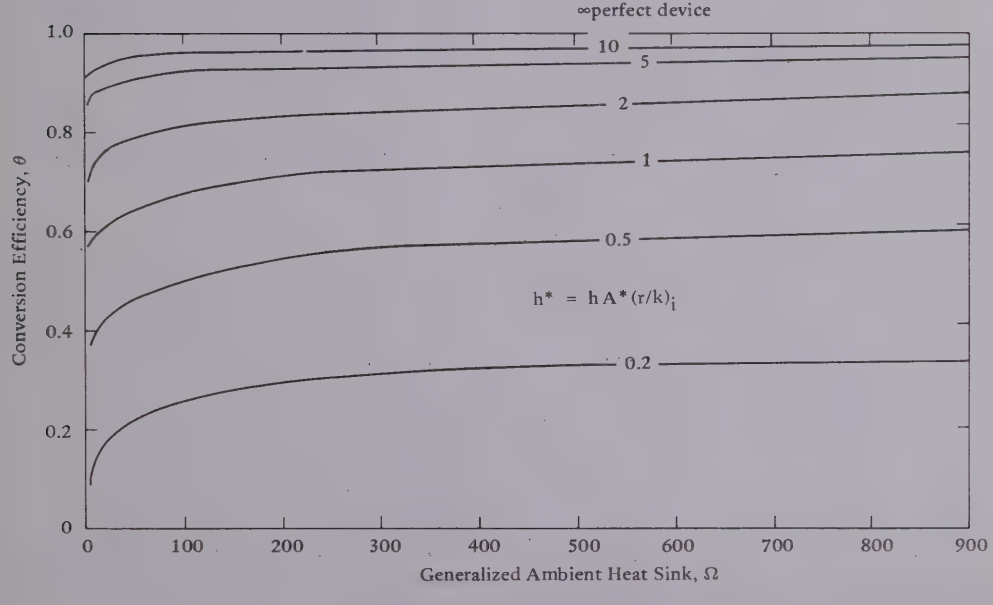

Figure 5. Freezing cell performance curves.

Equation 24 may be written in an alternative form

$$\Omega = \omega + \frac{\phi(\phi + 2)}{2h^*} \qquad (25)$$

which shows clearly that the ambient heat sink consists of a portion available and a portion unavailable for useful ice production.

Generalized Conductance

It may be noted that the formation of an annual ice sheet is a heat transfer problem similar to that of radial ice growth. In calculating the solidification rate of slab ice, it is necessary to know the history of ambient temperatures and the prevailing convective heat transfer coefficient at the air/sea-ice interface. Thus, the overall heat transfer coefficient in the present analysis is the freezing-cell counterpart to the convection coefficient encountered in problems of sheet ice growth.

Clearly, the performance of a freezing cell is a function of generalized conductance. The radius of the subsurface pipe r_i and the ratio of areas A^* of Equation 19 are fixed by design. The overall heat transfer coefficient, on the other hand, depends upon thermodynamic interaction: (1) heat rejection from the cooling head is enhanced by strong winds and (2) internal heat transport is facilitated by large temperature gradients, a well-circulating refrigerant, and a favorable diameter-to-length ratio. The overall heat transfer coefficient can always be established experimentally for a specific freezing cell by growing ice in laboratory or field. When air temperature and ice thickness are monitored, Equation 24 may be solved for h^*, and ultimately for h. However, such a procedure is not convenient nor feasible to do for each and every variation in freezing cell design. A better course of action involves analyzing a proposed design or configuration of freezing cell in terms of heat exchanger theory. In other words, each of the component thermal resistances designated in Equation 18 is evaluated; the sum total, of course, produces the overall heat transfer coefficient. To this end, well-established empirical relationships are employed to calculate the relative magnitude of each thermal resistance. A more detailed outline of a typical step-by-step design procedure is included in the example presented in the Appendix.

Heated Seawater

Equations presented heretofore in this publication predict radial ice growth in seawater that is at freezing point temperature, a condition which exists at strategic polar locations during the winter ice-growth period. However, it is recognized that in some coastal areas the seawater temperature may be temporarily elevated above the freezing point for a period of time. This condition is especially true during the post-winter melt period when heated surface run-off percolates into coastal waters. A mathematical analysis, supported by laboratory tests, was performed in order to specify quantitatively the interaction between ice growth and heated seawater.

Consider the shell of seawater ice that forms around a subcooled pipe. Heat transfer occurs in the very thin layer of water immediately surrounding a growing ice front. Heat is removed from this incremental volume by means of conduction through the ice shell into the cold pipe and, at the same time, if the seawater medium is above freezing, heat is added by means of convection. An energy balance at the ice/seawater interface provides the following qualitative relationship:

> Rate of heat conduction out minus rate of heat convection in equals rate of ice growth

This expression implies that convective heating effectively retards the rate of ice production. This is true, but in addition it limits the maximum thickness that can be achieved. For example, as an ice shell thickens and conduction decreases as insulation increases, a static point of no growth is eventually reached. If static conditions change, then heat transfer continues until a new equilibrium is established.

The energy balance as stated in the preceding paragraph may be expressed mathematically. The basic differential equation is Equation 14, except that now a new parameter expressing the dimensionless ratio of convection to conduction energy is introduced

$$\frac{dR}{d\Omega} = \frac{\theta}{R \ln(R)} - \frac{h_\infty r_i}{k_i} \theta_\infty \qquad (26)$$

for which h_∞ is the heat transfer coefficient between the ice shell and seawater, and θ_∞ is the temperature ratio of heating to cooling

$$\theta_\infty = \frac{\overline{T}_\infty(t) - T_\lambda}{T_\lambda - \overline{T_a(t)}} \qquad (27)$$

The new dimensionless quantity is defined as the convective heating modulus and is designated by the symbol h^{**}. Thus, by definition,

$$h^{**} = \frac{h_\infty r_i}{k_i} \theta_\infty \qquad (28)$$

and the shortened form of Equation 26 is

$$\frac{dR}{d\Omega} = \frac{1}{R \ln(R) + (R/h^*)} - h^{**} \qquad (29)$$

Equation 29 does not have an exact mathematical solution; however, it may be rewritten in a form that can be integrated numerically. When Equation 21 is substituted for conversion efficiency, the result is

$$\Omega = \sum \frac{R \ln(R) + (R/h^*)}{1 - h^{**}[R \ln(R) + (R/h^*)]} \Delta R \qquad (30)$$

Figure 6 presents the results of the numerical integration.

HISTORICAL REVIEW

The freezing cell emerged as the most suitable device for accelerating subsurface ice growth in remote and hostile coastal regions after an extensive study by CEL of alternative schemes. One alternative method, for instance, involved the high-pressure pumping of a liquid or gas at subfreezing temperatures below an ice sheet, thereby promoting ice growth by direct mixing. This cold-fluid injection method was shown to demand a very large input power in return for a small refrigerating effect.

In the ice-chip injection process, low salinity, relatively cold ice chips taken from a borrow pit would be injected below a sheet of ice. It was predicted that chips sufficiently cooled and rapidly injected would fuse together and effectively form a new layer. Bearing strength would increase immediately in response to increasing buoyancy. Indeed, laboratory tests conducted in the CEL cold chamber facility showed that cold chips fused readily. However, it was noted that flexure strength would increase only as the liquid between contiguous chips froze. However, the forecast also indicated that considerable equipment and man-effort would be required to produce, transport and transplant ice chips below an ice sheet [8].

The third scheme studied involved the use of a conventional vapor-compression refrigeration system to subcool a refrigerant which would be circulated through freeze-points placed in an ice sheet. It was known that such a system would promote fast freezing at any ambient condition; but again, high costs, continuous power requirements, and severe logistic difficulties were limiting factors. However, it was from this basic idea that the concept of the freezing cell was born.

Early Tests in Laboratory and Field

CEL initiated a test and development program during FY-69 when three types of freezing cell were evaluated in a specially-constructed, styrofoam-insulated deep freeze tank [9]. Two of the devices were conventional ground-cooling devices purchased from industry: the Balch cell, a liquid convection cell, and the Long cell, a two-phase, boiling liquid and convection cell. Each was constructed from 3-inch black pipe 7.5 feet long with longitudinal heat rejection fins. A specially constructed CEL cell, operating on the same principle as the Long cell, was designed with internal piping and a noninsulated flow divider to direct vapor and liquid to optimum heat exchange areas.

The results are presented in Figure 7 for the two test temperatures. As should be expected, the Long cell, which operates on a phase change, is less sensitive to decreases in ambient temperature than is the Balch cell, which operates on density differences.

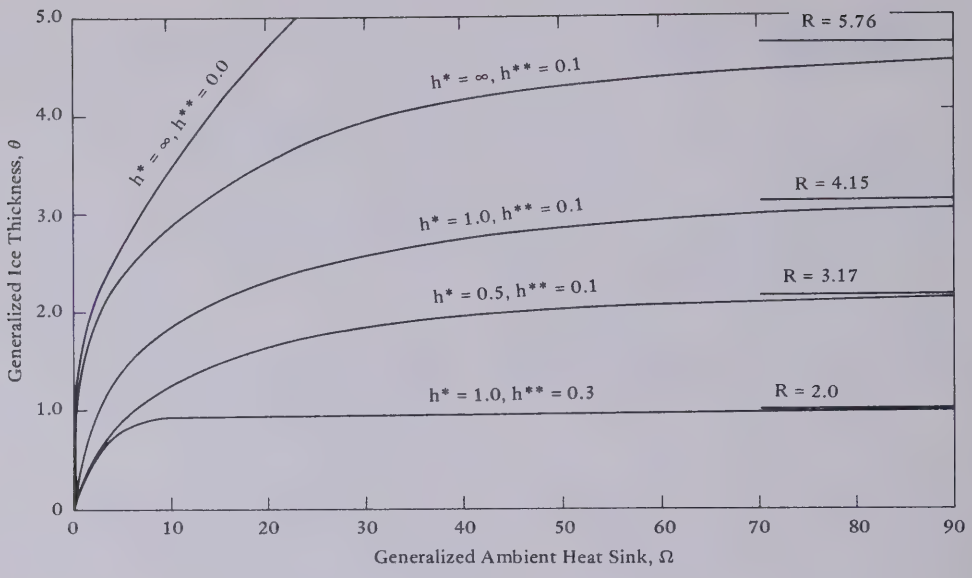

Figure 6. Dimensionless ice growth as a function of generalized conductance and convective heating.

As a result, the heat removal capacity of the two-phase cells was superior at 15°F, while the opposite was true at -30°F. It was concluded, therefore, that since the liquid convection cell was more effective at typical polar winter air temperatures and also functionally less complex, it should be the device to be further developed and tested in the field.

During March and April 1969, three Balch cells were monitored in the natural sea-ice near Point Barrow, Alaska. Two of the devices were made of 3-inch black iron pipe 12 feet long, while the third was made of 4-inch pipe 13 feet long. All three were charged with a 50-50 mixture of methyl alcohol and water. One of the 3-inch cells was instrumented with copper/constantan thermocouples for temperature measurement.

During operation, each cell with its adjoining section of natural ice sheet (Figure 8) was lifted periodically for visual inspection, ice growth measurement, and salinity determination. The two 3-inch devices produced an ice shell of 10.5-inch and 12.5-inch thickness after 25 and 32 days, respectively. The larger cell produced an ice shell thickness of nearly 14 inches after 28 days.

During FY-70, an attempt was made to construct two small, grounded, ice structures in the near-shore area off Point Barrow. Each freezing system consisted of seven liquid, convection, freezing cells arranged in a hexagon configuration. Each cell, in turn, was constructed from 4-inch, 13-foot-long pipe with internal ducts and insulated dividers to channel flow.

Both structures were placed in December when the sea ice was 38 inches thick and removed in May, 162 days later. Both ice structures were susceptible to cracking due to tidal movement. Although positioned 40 feet seaward from the tidal crack, cracking of the ice between cells soon began because the two shoreward cells in each structure were initially grounded. Additional cracking did not occur until later when the two seaward cells finally grounded. As before, grounding prevented bending, and thus cracking occurred [9].

One recommendation issued after the field tests was that, internally, freezing cells should be as simple as possible. It was noted that ducts and flow dividers did not appear to enhance performance; subsequent tests in the laboratory confirmed this observation. Thus, the present device of generation contains no internal plumbing.

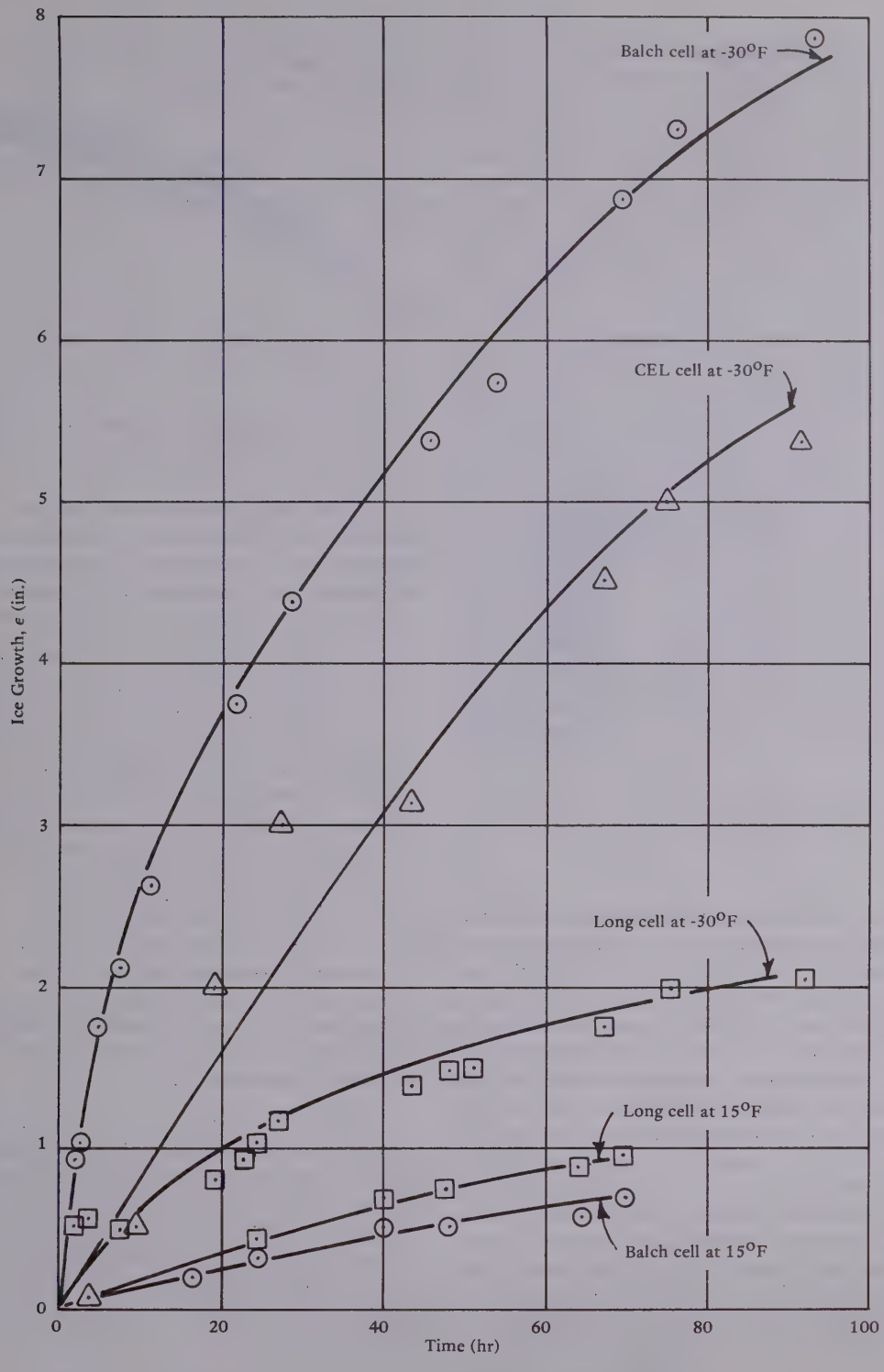

Figure 7. Evaluation of early freezing cell designs.

Figure 8. Freezing cell tested near Barrow, Alaska, during FY-69.

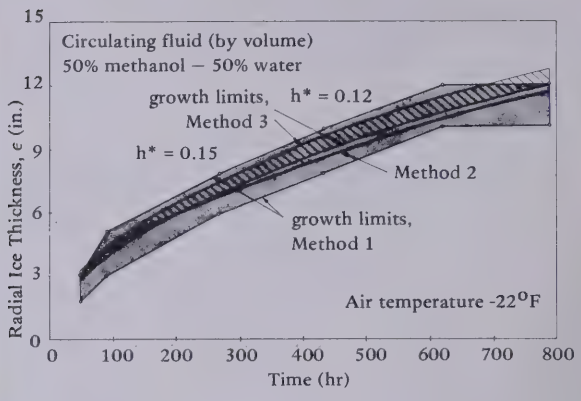

Figure 9. Radial ice growth around a 1-1/2-inch-diameter, 4-foot-long freezing cell.

The laboratory and field tests during FY-69 and FY-70 were conducted entirely on a try-and-see basis. The devices were placed, charged, and the ice thickness measured; however, no attempt was made to correlate this ice growth in terms of freezing cell design or specific temperature conditions. Thus, an analytical study was conducted, resulting in the working ice growth Equations 10 and 24. The reliability of these equations was established by a series of laboratory and field tests during FY-73 [6].

In the laboratory, freezing cells were tested using various solutions of calcium chloride and water or methyl alcohol and water as the circulating liquid. The cells were installed in pairs with a thin wire stretched in between. To these wires, thermocouples were fitted at measured intervals so that ice thickness could be monitored. While the exact position of the freezing front could not be determined using this method, it could at least be pinpointed as between two adjacent thermocouples. In this manner, there were three ways of designating ice thickness:

Method 1. Temperature readings from thermocouples along the connecting wires were used to plot actual ice thickness. In practice, actual ice thickness represented a zone of uncertainty since the freezing front at best could be located as somewhere between two neighboring thermocouples. Figure 9 is typical of the results obtained. Actual ice thickness is pictured as a shaded area between an upper and lower limit which corresponds, of course, to the radially more distant and less distant thermocouples, respectively.

Method 2. Thermocouples were also placed on the lower heat exchange surface of each cell to measure the thermal history. In this way, the effective heat sink was calculated, and Equation 10 evaluated for ice thickness. This thickness curve is presented in Figure 9 as a single line.

Method 3. Ice thickness was calculated directly from Equation 24. The ambient heat sink was calculated from air temperature data. Generalized conductance was established through heat transfer analysis: each cell was treated as a heat exchanger, and the various thermal resistances calculated. To facilitate this treatment, the heat rejection surface of each cell was made of unfinned tubing. This construction did not provide the optimum heat exchange

surface, but it provided a geometry for which the cooling head-to-air resistance could be calculated empirically. Even so, fluctuations in the air current pattern within the test chamber prevented an exact assessment. Therefore, two magnitudes of air current were used to calculate high and low values of generalized conductance. The range in between those limits is presented in Figure 9 as cross-hatched for emphasis.

The applicability of the analytical ice growth equations was established under field conditions during March and April 1973. At that time, six freezing cells were installed through the annual ice about 200 yards offshore near the Naval Arctic Research Laboratory, Barrow, Alaska. Two of the cells were charged with a mixture of 44% methyl alcohol (by weight) and water; an additional two were filled with antifreeze, Arctic type which by weight contains approximately 55% ethylene glycol and 32% water; the final two contained a calcium chloride brine solution. Each cell was an assembly of two pieces corresponding to the rejection and injection surfaces of the heat exchanger. The subsurface section was 16 feet long and constructed from either 2-inch-diameter wire-reinforced vinyl tubing or 2-inch-diameter galvanized pipe. The cooling head consisted of three (upright and parallel) 4-foot-lengths of 1-inch-diameter copper tubing with 2-inch (outside diameter) aluminum fins. Figure 10 shows the freezing cells at the test site.

The subsurface section of each heat exchanger was fitted with thermocouples to monitor pipe temperature. From these data the effective heat sink was calculated. Air temperatures were monitored continuously to evaluate the ambient heat sink. Figure 11 shows the resulting ice growth for each of the three pairs of freezing cell. Using Equations 24 to solve for h^*, the magnitude of generalized conductance varied between 0.12 and 0.14 for these systems.

Recent Tests in the Laboratory

The foregoing summary discussed laboratory and field results which have appeared in greater detail in earlier CEL publications. The laboratory studies to be presented now were conducted subsequent to 1973 and have not heretofore appeared in any technical document.

Heated Seawater. The FY-73 field tests at Barrow were conducted with the seawater at the freezing point. However, it was obvious that to fully understand the growth mechanism, it was necessary to consider the effects of a heated medium. Thus, the theoretical study presented in the Analysis section was conducted. In order to support that mathematical development, a test was conducted in the cold chamber facility at CEL. A portable refrigeration unit of 6,350-Btu/hr capacity was used to cool a reservior filled with Arctic-type antifreeze. The antifreeze, in turn, was pumped through pipes (freeze points) that had previously been placed in the seawater tank; however, pumping did not begin until after both the seawater and antifreeze were cooled to the selected test temperatures. Ice thickness was measured by means of thermocouple readout.

Figure 12 presents the experimental and numerically integrated curves for one test system. The freeze points consisted of 1-1/2-inch-diameter pipes positioned vertically such that the bottom 2-foot section was exposed to seawater. Average temperatures of 33°F for seawater and 15°F for antifreeze were maintained during the 74-hour trial. The test was discontinued because the front stopped (or nearly stopped) growing. The curves are presented in terms of actual ice thickness and time to facilitate interpretation.

To integrate Equation 30 numerically, it was necessary to know the magnitude of the convective melting modulus h^{**} defined by Equation 28. Actually, the only unknown in Equation 26 is the heat transfer coefficient at the interface h_∞. The value of this parameter may be established from empirical heat transfer considerations. Since the seawater in the test tank was not circulated or agitated, the basic heat transfer problem for the given test conditions involved free convection along the length of the vertical cylinders. An empirical equation defining heat transfer is the following [10].

$$h_\infty = 0.13 \frac{k_w}{l} (Gr\,Pr)^{1/3} \qquad (31)$$

This equation was evaluated by inserting the appropriate properties of seawater. The resulting value of h_∞ was 27 Btu/ft^2-hr-°F. Figure 12 shows that there is good agreement between the experimental and theoretical results.

Figure 10. Barrow test site on annual ice sheet.

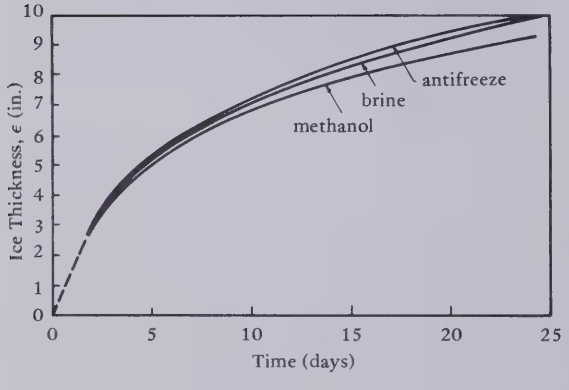

Figure 11. Radial ice growth around antifreeze, brine, and methanol charged cells.

Aluminum Cooling Head. The FY-73 field program in Alaska uncovered a problem inherent to cooling heads with small, finely spaced fins: drifting snow was easily entrapped and impacted in the spaces between fins. It had to be removed manually. A major directive of this research required the development of a lightweight, maintenance-free device. Thus, it became apparent that the best design would utilize large, continuous, longitudinal fins along the length of the cooling head. Therefore, several cooling heads constructed of aluminum tubing with welded-on aluminum plate fins were evaluated in the CEL cold chamber facility. The test procedure was as follows: the seawater was chilled to the phase-change temperature, the freezing cell was positioned and charged with Arctic-type antifreeze, and the facility was maintained at a select air temperature of -15°F. Thermocouples attached to the subsurface section of the heat exchangers were used to monitor pipe temperatures.

Each cooling head was constructed from 4-inch-diameter aluminum tubing 30 inches in height. Twelve, equally spaced, longitudinal fins made from 1/8-inch-thick aluminum plate were welded to each cooling head. Each fin was 24 inches high and 2-1/2 inches long (where fin length is the radial extension outward from the tubing to which the fin is attached). Thus, the total surface area of the cooling heads was 11 square feet. The overall fin efficiency calculated for the given configuration and environmental conditions was 0.95. Therefore, the effective area of each cooling head was 10.5 square feet.

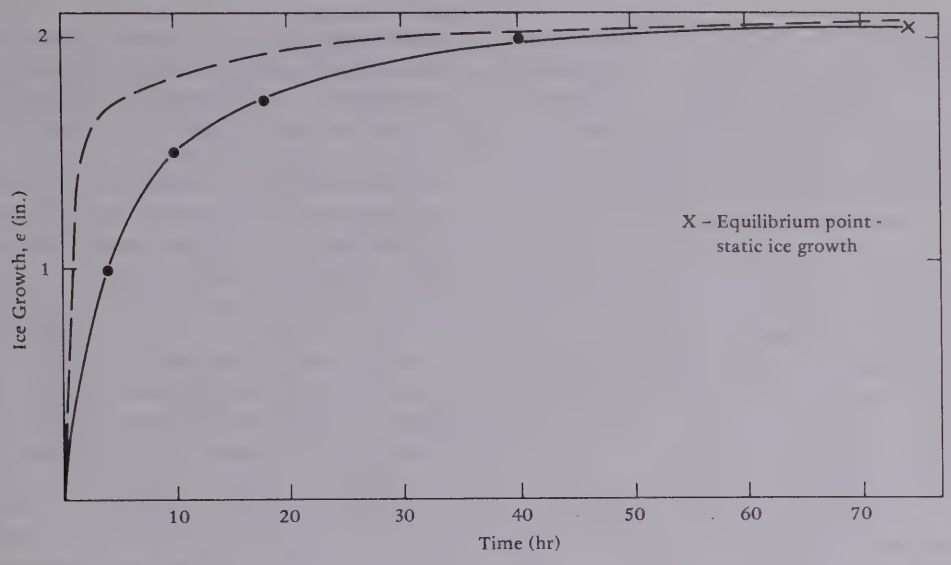

Figure 12. Ice growth in seawater at 33°F.

Generalized conductance, the parameter indicating heat exchanger performance, was calculated from ice growth data to vary between 0.5 and 0.54. Previous values of h* for freezing cells tested in the cold chamber and in Alaska ranged from 0.12 to 0.22. Thus, the increased fin performance of the aluminum cooling heads resulted in improved efficiency.

DISCUSSION

A freezing cell will operate as long as the following requirements are satisfied: (1) the ambient air temperature is below that of the seawater; (2) a section of heat exchanger is exposed to the ambient air (cooling head); (3) a section of heat exchanger is emerged in the warmer seawater (freeze pipe); and (4) a well-convecting, nonfreezing liquid is used for internal circulation. Any configuration which includes each of these factors will result in some degree of performance; however, it is only natural to conclude that specific combinations of materials and design will result in enhanced efficiency. For instance, it is intuitive, and obvious from Equations 19 and 20, that the ratio of cooling head to freeze pipe surface area directly affects the potential production of ice: the greater the heat exchange area exposed to air, the cooler will be the operating temperature of the liquid refrigerant. This heat rejection surface can be effectively increased by the addition of cooling fins. Of course, there are practical limits since the efficiency of a finned surface decreases steadily as the fin is extended radially outward. The specific pattern of the efficiency function is dependent upon thermal conductivity. Thus, material consideration in addition to size characteristics play an important role. In this respect, the choice of material for cooling head construction is more or less confined to one of the metals. Aluminum is especially suited since it has the properties of low density and high thermal conductivity. It is noted in the Appendix that for two cooling heads of equivalent weight and fin efficiency, one constructed of aluminum and the other of steel, the aluminum unit will have three times as great a surface area for cooling. Steel, on the other hand, is less expensive and more versatile to work with.

The material makeup of the subsurface freeze pipe is also important. It is assumed in the electrical analogue that the thermal resistance of the subsurface section is small and, therefore, it is not included in analysis. This assumption is readily true for metallic substances since the thermal conductivity is high and

the pipe thickness small; however, for other materials the resistance may need be considered. For instance, consider the wire-reinforced vinyl tubing tested at Barrow, Alaska. Although the thermal conductivity of the plastic material was low, the thermal resistance was still negligible because the membrane was so very thin. On the other hand, the vinyl plastic was very brittle and proved to be unsatisfactory at temperatures typical to polar regions. A stronger, more durable flexible hose material was tested in the CEL cold chamber. It consisted of wire-reinforced cotton fabric with a neoprene coating. In addition to the standard stock configuration, hoses with one and two extra coatings of neoprene were tested. Each of these specimens leaked between fabric and wire. Subsequent test sections with four coatings did not leak; however, the thermal resistance due to the thickened rubber shell was considerable. Heat transfer was severely restricted so that such rubber materials are not practical.

The degree to which fluid circulation interrupts effective heat transfer may be established by considering the material properties of various fluids. In the analysis of natural convection systems, the governing material properties are most usually grouped in terms of two dimensionless moduli, or similarity parameters. The Grashof number (Gr) represents the ratio of buoyant to viscous forces, and the Prandtl number (Pr) represents the ratio of momentum to thermal diffusivities. Thus, for any system dominated by natural convection circulation, it is expected that heat transfer will be functionally related to the relative magnitudes of these two dimensionless properties. Those liquids evaluated by CEL included water solutions of methyl alcohol and calcium chloride brine, as well as Arctic antifreeze. Neither of these fluids has a distinct advantage from a performance point of view; however, they may be rated according to other considerations. Anhydrous calcium chloride salt, for instance, is easily transported and readily mixed into solutions with freezing points as low as -50°C. On the other hand, field experience indicated that even optimum mixtures become gelatinous and highly viscous at prolonged temperatures below -40°C. The major disadvantage of methyl alcohol involves safety considerations: its high flammability and toxicity. It must be handled with care. Freezing cell systems proposed by CEL utilize Arctic antifreeze. This substance is pre-mixed for immediate use, easily and safely transported, and a common item at naval establishments in both the Arctic and Antarctic. The major limitation of this material is the recent surge in cost.

The freezing cell is a bounded system. As a result, internal heat transport is dependent upon geometry through the ratio of cell radius to length. The greater the ratio, the greater will be the liquid convection. It may be demonstrated, however, that this dependence is not usually a prime determinant of performance. In most instances, the thermal resistance of the cooling head is the greatest limitation to heat transfer so that a significant increase in liquid resistance (i.e., by a reduction in the radius-to-length ratio) does not appreciably alter the sum total of all resistances. In addition, it is shown in the Appendix by equation that the unit conductance of the circulating liquid is proportional to the fourth root of the radius-length ratio. Thus, a 16-fold decrease in the ratio results in just a 50% reduction in unit conductance (or synonymously, a 50% increase in liquid resistance).

Alternative configurations that satisfy the basic requirements for operation can be used in design. During FY-69, for instance, freezing cells shaped as continuous loops were tested in the CEL cold chamber. An uneven generation of buoyant forces in the two vertical legs of each device resulted in a general circulation around the entire loop. These loops, or horizontal cells, have great potential for use in areas where thay can be easily and effectively installed. Potential applications include reforming undercut ice embankments and bulk ice reclamation.

Freezing cells are by no means a panacea for large-scale ice-growth problems. They do have operational shortcomings. The most serious limitation is the decrease in growth rate with increased ice buildup. A growing ice shell undergoes a common fate as does an advancing ice sheet: the thickness that can be achieved in a winter season is limited by insulating effects. The second limitation involves cooling head design. Air is a poor conductor of heat. As a result, the performance of a freezing cell is severely handicapped. These devices are destined to have low percentages of conversion efficiency. Recent development and testing in the cold chamber facility at CEL has resulted in lightweight units with h^* values up to 0.5; however, even these improved values

are far less than that of infinity required for the perfect cell.

Of course, performance may be improved by increasing cooling head surface area; however, there are practical limits. Excessive increases in size counter the basic design requirement for lightweight, easily installed units. Furthermore, the functional relationship between conversion efficiency and generalized conductance is asymptotic, not linear, as is obvious from Equation 21 and Figure 5. Thus, an increase in A^* does not result in a proportional increase in θ, and the proportion that is realized becomes less and less for increasing values of h^*. In addition, the relationship between the effective heat sink and ice thickness is not linear. The greater the effective temperature potential, the more rapid will be the ice growth; but, as a result, the more rapid will be the decline in growth rate. To express it simply, the freezing cell becomes less productive more quickly. Less efficient freezing cells produce less ice in a given time period, but, at the same time, they undergo a less drastic decrease in growth rate. This is not to say, of course, that low efficiency cells are more desirable. It is always desirable to use as efficient a cell as is available. However, from the standpoint of material conservation and design objective, it may be advantageous to fabricate and install many lightweight, man-portable units as opposed to fewer heavy, more efficient units. An example is demonstrative. Consider freezing cells operating in air at an average temperature of -13°F. After 6 months, a (hypothetical) perfect cell of 6-inch pipe diameter would produce a thickened ice shell of 60 inches outside diameter. Smaller freezing cells of 2-inch pipe diameter, with h^* values of 0.5 and 0.2, would produce thickened ice shells of 38 and 32 inches, respectively. In terms of volume, that produced by one perfect device of 6-inch diameter can be equally well-produced by just two 2-inch cells with an h^* of 0.5, three 2-inch cells with an h^* of 0.2.

It becomes important, then, to achieve a compromise between heat transfer and size for a given application since freezing cells may be tailored to meet specific needs. One important consideration is ice-sheet thickening in remote, unmanned areas where power and construction equipment are not available. Figures 13 and 14 present in cross section and elevation, respectively, two typical cooling head designs suitable for remote assembly and installation. One is designed using steel and the other aluminum. Basic criteria used to establish cooling head characteristics are as follows: (a) weight of 50 pounds, (2) use of longitudinal fins, and (3) fin length so that efficiency at the end is 50%. The rationale used for each requirement is as follows:

(1) Work in desolate, unmanned areas of the polar regions must be performed using a minimum of power and equipment. The 50-pound limit of the cooling head is set as a weight that can be easily handled and placed by two men during installation procedures.

(2) The use of full-length, longitudinal fins along the cooling head reduces the possibility of snow becoming entrapped between fins, thereby minimizing the need for maintenance.

(3) The overall efficiency of a fin decreases as fin length is increased. The percentage decrease is dependent upon fin material and environmental conditions. A practical guide as to cost and weight is to limit the length to obtain an efficiency of 50% at the end of the fin.

SUMMARY

A major goal of this research was to produce a scheme for accelerating subsurface ice growth at select locations of a natural ice sheet using lightweight, man-portable equipment that can be easily assembled onsite by a minimum of personnel. Freezing cells provide a flexible method of achieving this goal.

Potential uses include the construction of platform foundations for winter facilities and quay areas for offloading ships. Other applications arise from the dynamics of ice under load. When subjected to stationary loads, ice will creep. Loads that can be accommodated safely by an ice sheet for short periods of time may cause failure on a long term basis.

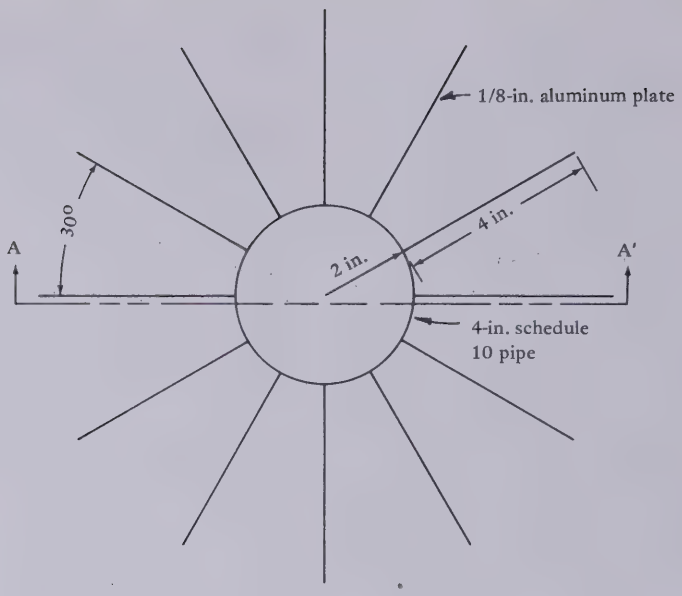

(a) Aluminum cooling head.

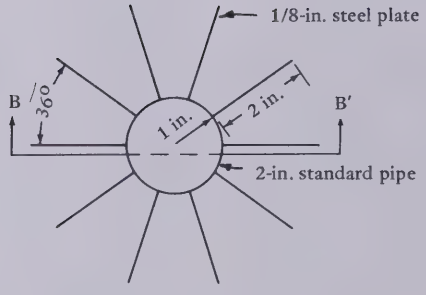

(b) Steel cooling head.

Figure 13. Cross-sectional view of typical cooling heads.

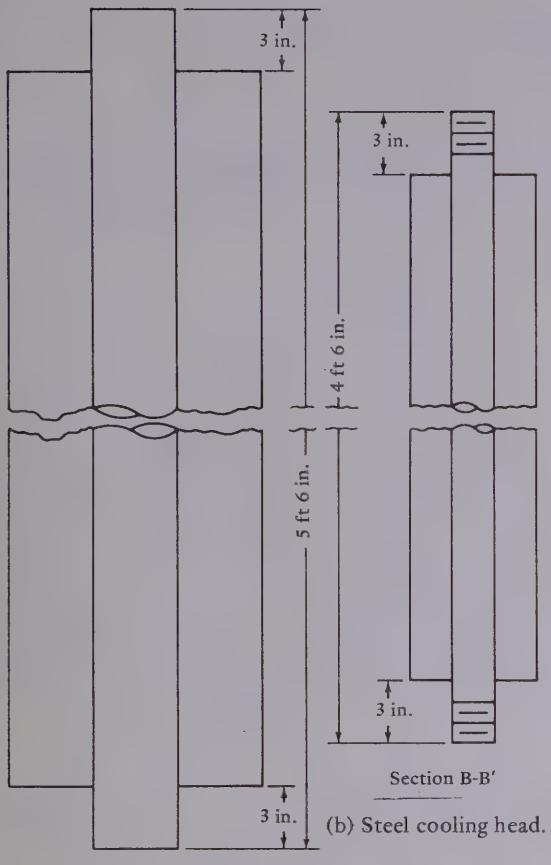

(a) Aluminum cooling head.

(b) Steel cooling head.

Figure 14. Elevation view of typical cooling heads.

REFERENCES

1. Civil Engineering Laboratory. Technical Note N-1376: The man-made McMurdo ice wharf – history, construction, and performance, by J. L. Barthelemy. Port Hueneme, CA, Feb 1975.

2. Naval Civil Engineering Laboratory. Technical Report R-185: Point Barrow trails, FY 1959: investigations of thickened sea ice, by J. E. Dykins and A. I. Funai. Port Hueneme, CA, Apr 1962. (AD 275502).

3. ———. Technical Report R-218: Point Barrow trails, FY 1970: Free flooded and ice-aggregate-fill, by J. E. Dykins, N. S. Stehle, and K. O. Gray. Port Hueneme, CA, Nov 1962. (AD 291698).

4. ———. Technical Report R-189: Sea ice engineering, summary report. Project ICE WAY, by W. D. Kingery, et al. Port Hueneme, CA, Sep 1962. (AD 287604). Also published as: Air Force Cambridge Research Laboratories. Report AFCRL-62-498; Air Force Surveys in Geophysics no. 145: Summary report-Project ICE WAY, edited by W. D. Kingery. Bedford, Massachusetts, May 1962. (AD 283984).

5. ———. Technical Report R-511: Ice construction: Methods of surface flooding, by C. R. Hoffman. Port Hueneme, CA, Jan 1967. (AD 645917).

6. Civil Engineering Laboratory. Technical Report R-811: Ice engineering-quantification of subsurface ice thickening techniques, by J. L. Barthelemy. Port Hueneme, CA, May 1974.

7. A. L. London and R. A. Seban. "Rate of ice formation," Transactions of the ASME, vol. 65 (1943), pp. 771-778.

8. Naval Civil Engineering Laboratory. Technical Note N-884: A preliminary subsurface heat transfer study of thickening sea ice, by E. R. Vineratos. Port Hueneme, CA, May 1967.

9. ———. Technical Note N-1078: Ice construction – investigation of accelerated bottom-freezing techniques, by C. R. Hoffman and T. L. Culbertson. Port Hueneme, CA, Feb 1970.

10. F. Krieth. Principles of heat transfer. Scranton, PA, International Textbook Co., 1959.

11. J. P. Holman. Heat transfer, 2nd Edition. New York, NY, McGraw-Hill, 1968.

12. G. O. Curme and F. Johnston. Glycols. New York, NY, Reinhold Publishing Corporation, 1952.

Appendix

SAMPLE CALCULATIONS

In this appendix, sample calculations are presented. A step-by-step procedure outlines methods for evaluating the ice growth equations quantitatively, and for analyzing the freezing cell as a heat exchanger. A hypothetical situation is considered. For convenience, winter conditions typical to the offshore area near Barrow, Alaska, are used. More specifically, average air temperature and windspeed of -10°F and 10 mph, respectively, are assumed.

Suppose, for sake of example, it is desired to place a row of freezing cells at a remote offshore site such that, at the end of a 6-month growth period, the subsurface ice growths of adjacent cells will touch one another. (In a real situation this criteria may or may not be necessary, depending on the distribution and intensity of the surface load.) In the design of such a system, it is necessary to estimate final radial ice thickness in order to calculate proper freezing-cell spacing. Equation 24 applies

$$\omega = \frac{1}{2}(\phi + 1)^2\left[\ln(\phi + 1) - \frac{1}{2}\right] + \frac{\phi(\phi + 2)}{2h^*} \qquad (24)$$

The left side of this equation represents the generalized ambient heat sink and is defined by Equation 11

$$\Omega = \frac{\alpha}{r_i^2}\left[T_\lambda - \overline{T_a(t)}\right]t \qquad (11)$$

The constant α contains ice properties which are assigned the following average values, where $\alpha = (k/\rho L)_i$

ρ_i = 56 lb/ft^3

k_i = 1.15 Btu/ft-hr-°F

L_i = 140 Btu/lb

The number of degree-hours of frost is based on an average air temperature of -10°F, a seawater temperature of 29°F, and a growth period of 180 days; therefore,

$$[T_\lambda - \overline{T_a(t)}]\,t = (29 + 10)(180)(24)$$

$$= 168{,}500\,^{\circ}\text{F-hr}$$

Since the site is remote, it is desired to use lightweight systems that can be installed by two men. Two configurations of cooling head, as diagrammed in Figures 13 and 14 of the text, are considered. Let the subsurface freeze pipe for each configuration extend 15 feet below the top of the ice sheet. Four-inch-diameter aluminum pipe is used for the aluminum cooling head and 2-inch-diameter steel pipe for the steel head. For the aluminum head,

$$r_i = 1/6 \text{ ft}$$

and for the steel head

$$r_i = 1/12 \text{ ft}$$

Substituting values into Equation 11 gives magnitudes for each of the configurations

$$\Omega(\text{aluminum}) = \frac{(1.15)(6)^2}{(140)(56)}(168{,}500) = 890$$

$$\Omega(\text{steel}) = \frac{(1.15)(12)^2}{(140)(56)}(168{,}500) = 3{,}560$$

Thus, Equation 24 is reduced to two unknowns, dimensionless ice thickness (ϕ) and generalized conductance (h^*). The latter quantity must be determined by studying the two freezing cell designs in terms of heat exchanger theory.

The overall heat transfer coefficient (used to determine h^*) for each configuration is determined by summing each of the thermal resistances given in Equation 18

$$R_1 + R_2 + R_a = \frac{1}{h A_a} \qquad (18)$$

It is expected that R_a, the resistance between air and cooling head, will dominate; therefore, it is calculated first. In terms of heat transfer parameters, R_a may be rewritten as

$$R_a = \frac{1}{\eta (h A)_a}$$

where A_a is the total surface area of the cooling head and h_a is the unit conductance to the air. The latter quantity may be determined by a standard empirical heat transfer relationship [11].

$$\frac{h_a D_a}{k_a} = 0.024 \left(\frac{V D}{\nu} \right)_a^{0.805}$$

where $D_a = 2r_i$

V_a = 10 mph (15 ft/sec)

$\nu_a = 1.18 \times 10^{-4}$ ft^2/sec

k_a = 0.012 Btu/ft-hr-^{o}F

Substitution of values and solution for h_a gives

$$h_a(\text{aluminum}) = 4.6 \text{ Btu/ft}^2\text{-hr-}^o\text{F}$$

$$h_a(\text{steel}) = 4.3 \text{ Btu/ft}^2\text{-hr-}^o\text{F}$$

The parameter η in the equation for R_a denotes the overall efficiency of the fin configurations. As indicated in Figure 15, both configurations were designed to give an overall fin efficiency of about 80%. Since the surface areas of the aluminum and steel cooling heads are 43 square feet and 15 square feet, the values of R_a are calculated to be

$$R_a(\text{aluminum}) = \frac{1}{(0.8)(4.6)(43)} = 0.006 \text{ Btu/hr-}^o\text{F}$$

$$R_a(\text{steel}) = \frac{1}{(0.8)(4.3)(15)} = 0.019 \text{ Btu/hr-}^o\text{F}$$

The internal resistances due to liquid circulation are also calculated from empirical relationships. Consider the resistance due to convective cooling in the cooling head. This resistance, denoted in Equation 18 as R_1, is written in standard heat transfer format as

$$R_1 = \frac{1}{h_f A}$$

The internal surface area of the cooling head is A, equal to 5.8 square feet for the aluminum device and 2.4 square feet for the steel device. The unit conductance h_f is calculated from the following empirical equation [11]

$$\frac{h_f r_i}{k_f} = 0.42 (\beta \, \text{Gr Pr})^{1/4}$$

where β is the ratio of cooling-head radius to freezing cell length

$$\beta(\text{aluminum}) = \frac{1/3 \text{ ft}}{20.5 \text{ ft}} = 0.016$$

$$\beta(\text{steel}) = \frac{1/6 \text{ ft}}{19.5 \text{ ft}} = 0.009$$

The product of the Grashof (Gr) and Prandtl (Pr) numbers provides the following relationship

$$\text{Gr Pr} = \left(\frac{C \rho^2 \tau g}{\mu k} \right) r^3 \Delta T$$

The liquid properties are assigned the following values [12] assuming that the liquid refrigerant is arctic-type antifreeze (60% ethylene glycol by weight).

C = 0.7 Btu/lb-^{o}F specific heat

k = 0.22 Btu/ft-hr-^{o}F thermal conductivity

ρ = 67.4 lb/ft^3 density

μ = 1 lb/ft-hr viscosity

τ = 0.00034/^{o}F coefficient of expansion

g = 32.2 ft/sec^2 gravitational constant

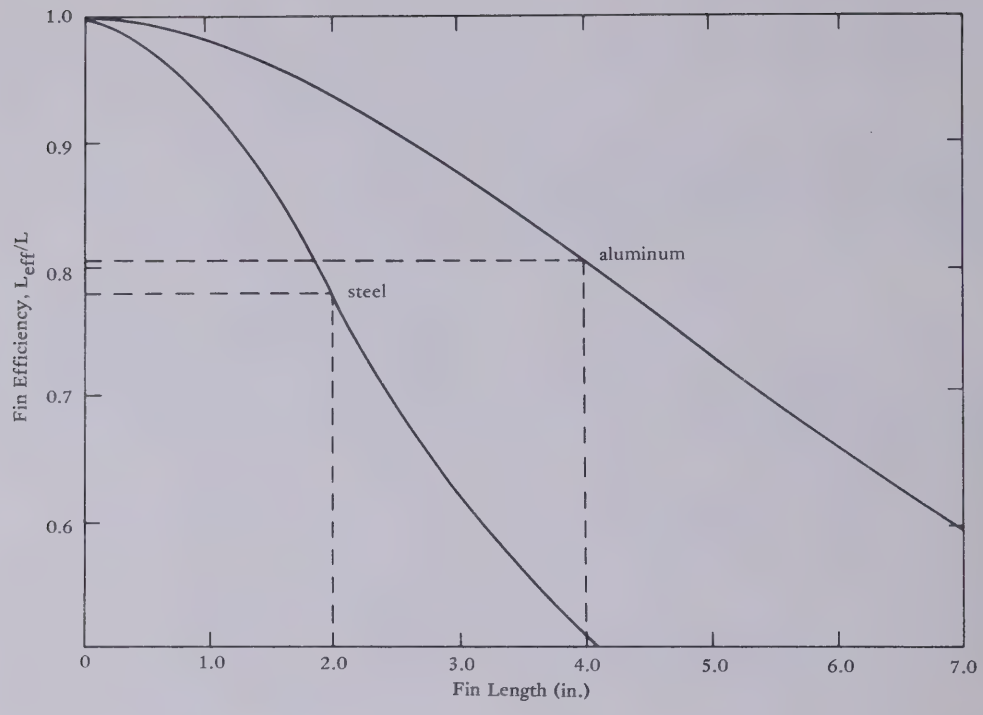

Figure 15. Overall fin efficiency as a function of fin length for 1/8-inch-thick aluminum and steel fins in a 10-mph wind.

The quantity ΔT reflects the temperature gradient across the liquid interface. It is constantly changing; however, a value can be assigned for computation without appreciable error. Let

$$\Delta T = 10^{o}F$$

Substitution of property values gives

$$Gr\,Pr(aluminum) = 9.2 \times 10^{7}$$

$$Gr\,Pr(steel) = 1.2 \times 10^{7}$$

which upon substitution into the basic equation for h_f gives

$$h_f(aluminum) = 19.3\ Btu/ft^2\text{-}hr\text{-}^{o}F$$

$$h_f(steel) = 19.0\ Btu/ft^2\text{-}hr\text{-}^{o}F$$

When these values are put into the relationship for R_1, the following resistance values result

$$R_1(aluminum) = \frac{1}{(19.3)(5.8)} = 0.009\ Btu/^{o}F\text{-}hr$$

$$R_1(steel) = \frac{1}{(19)(2.4)} = 0.021\ Btu/^{o}F\text{-}hr$$

For this design the original assumption was incorrect (that is, the liquid resistance is actually somewhat larger than that of cooling to the air).

The resistance due to liquid heating in the subsurface freeze pipe can also be calculated

$$R_2 = \frac{1}{h_f A'}$$

The area A' is the surface area inside the freeze pipe equal to 15.7 square feet and 7.9 square feet for the

aluminum and steel heads, respectively. It is safe to assume that the same values for h_f as previously calculated are reliable. Therefore,

$$R_2(\text{aluminum}) = \frac{1}{(19.3)(15.7)}$$

$$= 0.003 \text{ (Btu/}^{o}\text{F-hr)}^{-1}$$

$$R_2(\text{steel}) = \frac{1}{(19)(7.9)} = 0.007 \text{ (Btu/}^{o}\text{F-hr)}^{-1}$$

Now the overall conductance can be calculated, using Equation 18, for aluminum

$$0.009 + 0.003 + 0.006 = \frac{1}{h(43)}$$

$$h = 1.3 \text{ Btu/ft}^2\text{-hr-}^{o}\text{F}$$

and for steel

$$0.019 + 0.21 + 0.007 = \frac{1}{h(15)}$$

$$h = 1.4 \text{ Btu/ft}^2\text{-hr-}^{o}\text{F}$$

Finally, Equation 19 is used to find the values of generalized conductance

$$h^* = \left(\frac{r}{k}\right)_i h A^* \qquad (19)$$

$$h^*(\text{aluminum}) = \left(\frac{1/6}{1.15}\right)(1.3)\left(\frac{43}{15.7}\right) = 0.51$$

$$h^*(\text{steel}) = \left(\frac{1/12}{1.15}\right)(1.4)\left(\frac{15}{7.9}\right) = 0.19$$

Now the only unknown in the original Equation 24 is dimensionless thickness ϕ. This number may be determined by successive trial-and-error iteration. When this is done

$$\phi(\text{aluminum}) = 19$$

$$\phi(\text{steel}) = 28.6$$

In terms of actual thickness of ice,

$$\epsilon = \phi r_i$$

$$\epsilon(\text{aluminum}) = 19(2) = 38 \text{ inches}$$

$$\epsilon(\text{steel}) = 28.6(1) = 28.6 \text{ inches}$$

Thus, it would be necessary to give the aluminum cells an initial spacing of approximately 6.5 feet, and the steel cells a spacing of 5 feet.

LIST OF SYMBOLS

A	Surface area (ft^2)
C	Specific heat (Btu/lb-^oF)
D	Diameter of cooling head (without fins)
g	Gravitational constant (ft/sec^2)
h	Overall heat transfer coefficient (Btu/ft^2)
h_a, h_f, h_∞	Unit conductances (Btu/ft^2)
k	Thermal conductivity (Btu/ft-hr-^oF)
L	Heat of fusion (Btu/lb)
l	Length of freeze pipe (ft)
R_a, R_i, R_1, R_2	Thermal resistances
r	Radius (ft)
T	Temperature (^oF)
$\overline{T}$	Time-averaged temperature (^oF)
t	Time (hr)
V	Velocity (ft/sec)
α	Ice property constant, $(k/\rho L)_i$
β	Radius-to-length ratio
ϵ	Radial ice thickness, $r_o - r_i$
η	Fin efficiency
μ	Dynamic viscosity (lb/ft-sec)
ν	Kinematic viscosity (ft^2/sec)
ξ	Dummy variable of integration
ρ	Density (lb/ft^3)
τ	Coefficient of thermal expansion (per ^oF)

Dimensionless Moduli

$A^* = A_a/A_i$	Area ratio
Gr	Grashof number
$h^* = (r/k)_i h A^*$	Generalized conductance
$h^{**} = (r/k)_i (h\theta)_\infty$	Convective heating modulus
Pr	Prandtl number
$R = r_o/r_i$	Generalized radius
$\theta = \dfrac{T_\lambda - \overline{T}_i}{T_\lambda - T_a}$	Conversion efficiency
$\theta_\infty = \dfrac{T_\infty - T_\lambda}{T_\lambda - T_a}$	Convective heating ratio
$\phi = R - 1$	Generalized ice thickness
$\Omega = \dfrac{\alpha}{r_i^2}(T_\lambda - \overline{T}_a)t$	Generalized ambient heat sink
$\omega = \dfrac{\alpha}{r_i^2}(T_\lambda - \overline{T}_i)t$	Generalized effective heat sink

Subscripts

a	Air property; air/cooling-head interface
f	Liquid refrigerant
i	Ice property; freeze-pipe/ice-shell interface
o	Seawater/ice-shell interface
w	Property of seawater
λ	Phase change conditions
∞	Heated seawater conditions

DISTRIBUTION LIST

SNDL Code	No. of Activities	Total Copies	
—	1	12	Defense Documentation Center
FKAIC	1	10	Naval Facilities Engineering Command
FKNI	6	6	NAVFAC Engineering Field Divisions
FKN5	9	9	Public Works Centers
FA25	1	1	Public Works Center
—	6	6	RDT&E Liaison Officers at NAVFAC Engineering Field Divisions
—	92	94	CEL Special Distribution List No. 12 for persons and activities interested in reports on Polar Engineering